

Study of the molecular mechanisms driving the microgels behaviour through Raman spectroscopy and Dynamic Light Scattering

Valentina Nigro^{b,a}, Francesca Ripanti^{a,*}, Roberta Angelini^{b,a,*}, Angelo Sarra^a, Monica Bertoldo^c, Elena Buratti^c, Paolo Postorino^{a,*}, Barbara Ruzicka^{b,a}

^a*Dipartimento di Fisica, Sapienza Università di Roma, P.le Aldo Moro 5, 00185 Roma, Italy*

^b*Istituto dei Sistemi Complessi del Consiglio Nazionale delle Ricerche (ISC-CNR), sede Sapienza, Pz.le Aldo Moro 5, I-00185 Roma, Italy*

^c*Istituto per i Processi Chimico-Fisici del Consiglio Nazionale delle Ricerche (IPCF-CNR), Area della Ricerca, Via G.Moruzzi 1, I-56124 Pisa, Italy*

Abstract

Responsive microgels based on poly(N-isopropylacrylamide) (PNIPAM) exhibit peculiar behaviours due to the competition between the hydrophilic and hydrophobic interactions of the constituent networks. The interpenetration of poly-acrylic acid (PAAc), a pH-sensitive polymer, within the PNIPAM network to form Interpenetrated Polymer Network (IPN) microgels, affects this delicate balance and allows to control the temperature dependence of their typical Volume-Phase Transition (VPT) leading to complex behaviours whose molecular nature is still completely unexplored.

Here we investigate the molecular mechanism driving the VPT and its influence on particle aggregation for PNIPAM and IPN microgels by the joint use of Dynamic Light Scattering and Raman Spectroscopy. Our results highlight that microgel hydrophobicity is enhanced by the interpenetration of PAAc promoting interparticle interactions. Moreover we find that for IPN microgels two different molecular mechanisms drive the structural changes across the VPT, the first involving the coil-to-globule transition typical of the NIPAM chains and the latter driving the aggregation process supposedly due to the overexposure of the AAc chains. Finally a crossover concentration is found above which aggregation phenomena become relevant.

Keywords: Microgels - Swelling behaviour - Raman Spectroscopy - Dynamic Light Scattering

1. Introduction

Responsive microgels are highly attractive systems for several technological applications due to their high responsiveness to slight changes of environmental conditions [1]. Smart microgels have indeed

*Corresponding authors: francesca.ripanti@uniroma1.it (F.Ripanti); roberta.angelini@roma1.infn.it (R.Angelini); paolo.postorino@roma1.infn.it (P.Postorino)

many applications in agriculture, construction, cosmetics and pharmaceuticals industries, in artificial organs, and tissue engineering [2–7]. Moreover they are widely investigated in fundamental physics as good model systems for understanding the complex behaviours of soft colloids [8–10]. Their inter-particle potential and their effective volume fraction can be indeed modulated through easily accessible control parameters driving the system to unconventional phase-behaviours [11–14], drastically different from those of conventional hard colloidal systems [15–22].

In the last years, poly(N-isopropylacrylamide) (PNIPAM) has become very popular due to its thermo-sensitivity [23], induced by the competition between hydrophilic and hydrophobic nature of NIPAM chains across the Lower Critical Solution Temperature (LCST). At room temperature the polymer is hydrophilic and strongly hydrated in solution, while it becomes hydrophobic above 305 K, leading to a coil-to-globule transition that gives rise to a Volume-Phase Transition (VPT) from a swollen to a shrunken state of any PNIPAM-based microgel [24]. An increasing number of experimental [25–27] and theoretical [28–32] works aimed to describe this phenomenon. The typical swelling/shrinking behaviour affects particles interactions and drives the system towards unusual phase behaviours [1, 11, 12, 33, 34], controlled by changing concentration [11, 35], solvents [36], internal structure and composition (such as number and distribution of cross-linking points [27, 37] and core-shell structure [38, 39]) or by introducing additives into the PNIPAM network [38].

This mechanism can be even more complex if pH-sensitive polymers are introduced within the PNIPAM network, allowing to tune the polymer/polymer and polymer/solvent interactions. In particular the introduction of poly-acrylic acid (PAAc) to the PNIPAM microgel permits to control the temperature dependence of the VPT by pH [40–45], PAAc content [46, 47] or ionic strength [40, 48]. The response of PNIPAM/PAAc microgels is strictly related to the mutual interference between the two monomers [39–41, 43, 48–51]. In the case of interpenetration of hydrophilic PAAc into PNIPAM (PNIPAM-PAAc IPN microgel) [42, 46, 52–55] the coil-to-globule transition temperature of PNIPAM chains is almost unchanged [47], since irreversible chemical bonds between PNIPAM and PAAc chains are mainly excluded. This leaves the VPT temperature almost the same for PNIPAM and IPN microgels.

Up to now the driving forces for swelling have been estimated from the properties of linear PNIPAM in solutions leading to an entropically-driven, cooperative dehydration of the hydrophilic amide and hydrophobic groups [56–58], however a clear picture of the molecular mechanism behind swelling is still missing. To this aim Raman spectroscopy represents a powerful tool to highlight molecular changes related to the swelling behaviour as previously reported for PNIPAM microgels [56–58]. In the case of IPN microgels the delicate balance between hydrophilic and hydrophobic interactions is

affected by PAAc, leading to even more complex behaviours whose molecular nature has not been investigated up to now.

In this work we report for the first time the structural changes of PNIPAM and IPN microgels across the volume phase transition obtained through the joint use of Dynamic Light Scattering (DLS) and Raman Spectroscopy techniques. We find the molecular changes associated to the VPT for low concentration samples and to the aggregation for high concentration ones.

2. Experimental Methods

2.1. Sample preparation

Materials N-isopropylacrylamide (NIPAM) from Sigma-Aldrich and N,N'-methylene-bis-acrylamide (BIS) from Eastman Kodak were purified by recrystallization from hexane and methanol, respectively, dried under reduced pressure (0.01 mmHg) at room temperature and stored at 253 K until used. Acrylic acid (AAc) from Sigma-Aldrich was purified by distillation (40 mmHg, 337 K) under nitrogen atmosphere in the presence of hydroquinone and stored at 253 K. Sodium dodecyl sulfate (SDS), purity 98 %, potassium persulfate (KPS), purity 98 %, ammonium persulfate (APS), purity 98 %, N,N,N',N'-tetramethylethylenediamine (TEMED), purity 99 %, ethylenediaminetetraacetic acid (EDTA), and NaHCO₃, were all purchased from Sigma-Aldrich and used as received. Ultrapure water (resistivity: 18.2 MΩ/cm at 298 K) was obtained with Millipore Direct-Q® 3 UV purification system. All other solvents were RP grade (Sigma Aldrich) and were used as received. Before use, dialysis tubing cellulose membrane, cut-off 14,000 Da, from Sigma-Aldrich, was washed for 3 h in running distilled water, treated at 343 K for 10 min into a solution containing a 3.0 % weight concentration of NaHCO₃ and 0.4 % of EDTA, rinsed in distilled water at 343 K for 10 min and finally in fresh distilled water at room temperature for 2 h.

Synthesis of PNIPAM and IPN microgels PNIPAM micro-particles were synthesized by precipitation polymerization with (24.162 ± 0.001) g of NIPAM, (0.4480 ± 0.0001) g of BIS and (3.5190 ± 0.0001) g of SDS solubilized in 1560 mL of ultrapure water and transferred into a 2000 mL four-necked jacketed reactor equipped with condenser and mechanical stirrer. The solution was deoxygenated by bubbling nitrogen inside for 1 h and then heated at (343.0 ± 0.1) K. (1.0376 ± 0.0001) g of KPS (dissolved in 20 mL of deoxygenated water) was added to initiate the polymerization and the reaction was allowed to proceed for 16 h. The resultant PNIPAM microgel was purified by dialysis against distilled water with frequent water change for 2 weeks. In the second step IPN microgels were synthesized by a

sequential free radical polymerization method [42] with (140.08 ± 0.01) g of the PNIPAM dispersion at the final weight concentration of 1.06 %. 5 mL of AAc was copolymerized with (1.1080 ± 0.0001) g of BIS into the preformed PNIPAM microparticles at temperature in the range $293 \div 295$ K, where PNIPAM particles are swollen allowing the growth of the PAAc network inside them. The mixture was diluted with ultrapure water up to a volume of 1260 mL and transferred into a 2000 mL four-necked jacketed reactor kept at (294 ± 1) K by circulating water and deoxygenated by bubbling nitrogen inside for 1 h. 0.56 mL of TEMED were added and the polymerization was started with (0.4447 ± 0.0001) g of ammonium persulfate. Three different samples were prepared at three PAAc/PNIPAM ratio composition by stopping the reaction at the suitable degree of conversion of AAc. In the following we will refer to the weight concentration (%) of PAAc within each IPN microgel as C_{PAAc} . The obtained IPN microgels at the final PAAc concentration of $C_{PAAc} = 23\%$ were purified by dialysis against distilled water with frequent water change for 2 weeks, lyophilized and redispersed again in H_2O to obtain the final suspension at the required weight concentration. Samples at different weight concentrations, in the following referred as C_w , were obtained by dilution in H_2O .

2.2. Dynamic Light Scattering

Dynamic Light Scattering (DLS) measurements have been performed with a light scattering setup, where a monochromatic and polarized beam emitted from a solid state laser (100 mW at $\lambda = 642$ nm) is focused on the sample placed in a cylindrical VAT for index matching and temperature control. The scattered intensity is collected by single mode optical fibers at fixed scattering angles, namely $\theta = 90^\circ$, corresponding to $Q = 0.018 \text{ nm}^{-1}$, according to the relation $Q = (4\pi n / \lambda) \sin(\theta/2)$. The information on the system dynamics are extrapolated from the normalized intensity autocorrelation function $g_2(Q, t) = \langle I(Q, t)I(Q, 0) \rangle / \langle I(Q, 0) \rangle^2$, directly measured through DLS with a high coherence factor close to the ideal unit value. Measurements have been performed on aqueous suspensions of PNIPAM and IPN microgels at fixed PAAc content ($C_{PAAc} = 23\%$) as a function of temperature in the range $T = (293 \div 313)$ K, at four weight concentrations ($C_w = 0.1\%$, $C_w = 0.3\%$, $C_w = 0.5\%$ and $C_w = 0.8\%$) and pH 5.5. Reproducibility has been tested by repeating measurements several times.

As usual for colloidal systems, the intensity correlation functions are well described by the Kohlrausch-Williams-Watts expression [59, 60]:

$$g_2(Q, t) = 1 + b[(e^{-t/\tau})^\beta]^2 \quad (1)$$

where b is the coherence factor, τ is an "effective" relaxation time, defining the decay constant $\Gamma(Q) = 1/\tau(Q)$, and β describes the deviation from the simple exponential decay ($\beta = 1$) usually found in monodisperse systems and gives a measurement of the relaxation times distribution due to the intrinsic sample polydispersity. Many glassy materials show a stretching of the correlation functions (here referred to as "stretched behaviour") characterized by an exponent $\beta < 1$. Hydrodynamic radii R_H have been determined from the decay constant $\Gamma(Q) = Dq^2$ obtained through the analysis of the intensity correlation functions $g_2(Q, t)$ in the high dilution limit ($C_w = 0.1$ %).

2.3. Raman Spectroscopy

Raman measurements have been carried out using a Horiba HR-Evolution microspectrometer in backscattering geometry, equipped with a He-Ne laser, $\lambda = 632.8\text{ nm}$ and 30 mW output power ($\sim 15\text{ mW}$ at the sample surface). The elastically scattered light was removed by a state-of-the-art optical filtering device based on three BragGrate notch filters [61] which also allows to collect Raman spectra at very low frequencies (down to 10 cm^{-1} from the laser line). The detector was a Peltier-cooled charge-coupled device (CCD) and the resolution was better than 3 cm^{-1} thanks to a 600 grooves/mm grating with 800 mm focal length. The spectrometer was coupled with a confocal microscope supplied with a set of interchangeable objectives with long working distances and different magnifications ($20\times - 0.35\text{ NA}$ was used for the present experiment). Further details on the experimental apparatus can be found in [62]. Measurements have been performed on aqueous suspensions of PNIPAM and IPN microgels at fixed PAAc concentration ($C_{PAAc} = 23$ %) in the temperature range $T = (293 \div 313)$ K across the VPT, at two weight concentrations ($C_w = 0.3$ % and $C_w = 0.5$ %) and pH 5.5.

3. Results and Discussions

The size, the swelling behaviour and the dynamical changes of PNIPAM and IPN microgels across the VPT were assessed by DLS. In Fig.1 the relaxation time and the stretching parameter are reported as a function of temperature at four weight concentrations ($C_w = 0.1$ %, $C_w = 0.3$ %, $C_w = 0.5$ % and $C_w = 0.8$ %) as obtained through DLS by fitting the $g_2(Q, t)$ with Eq.(1).

A clear change of $\tau(T)$ and β parameters across the VPT is observed for both PNIPAM and IPN microgels (Fig.1). In the case of pure PNIPAM (Fig.1(a)) the well known dynamical transition associated to the VPT is evidenced [25, 44]: as temperature increases the relaxation time $\tau(T)$ slightly decreases up to the volume phase transition temperature above which it decreases to its lowest value, corresponding to the shrunken state indicating a fastening of the dynamics related to the reduced size

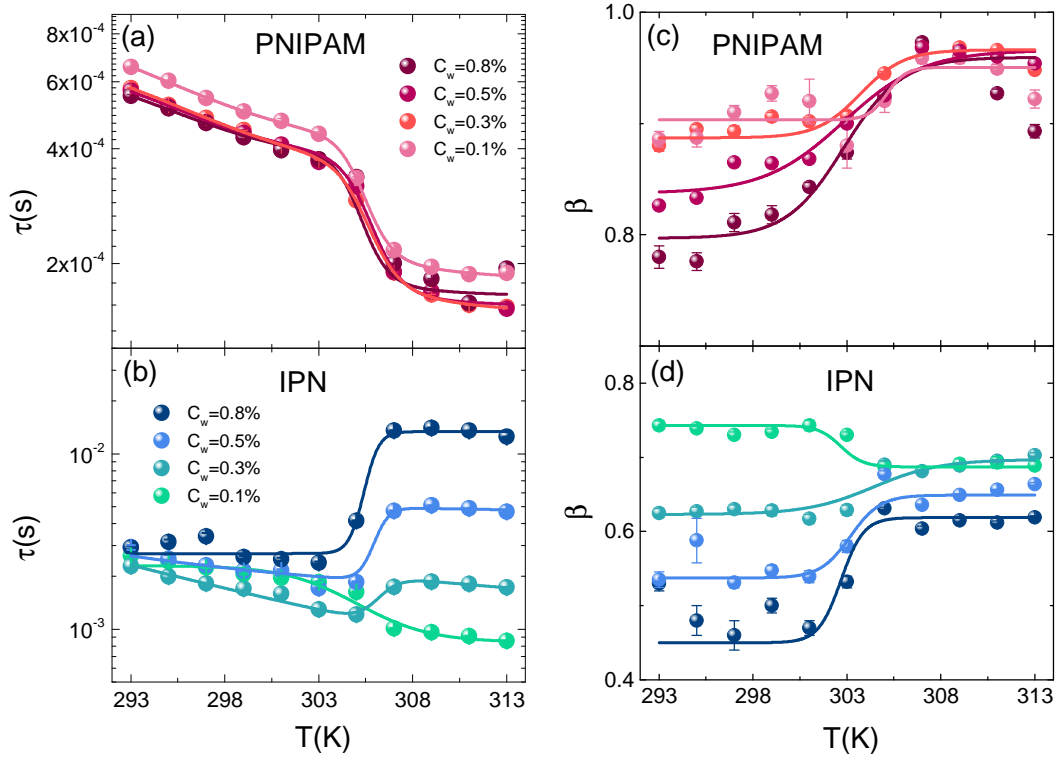


Figure 1: (a,b) Relaxation time and (c,d) stretching parameter as a function of temperature for PNIPAM and IPN microgels at $C_{PAAc}=23$ % at the indicated weight concentrations. Solid lines are guides to eyes.

of the particles. Moreover it decreases at increasing C_w , according to theoretical works predicting an increase of the diffusion coefficient with concentration [63, 64].

In the case of IPN microgels a different scenario shows up (Fig.1(b)), the relaxation time above the VPTT is strongly affected by weight concentration: while at low C_w it is similar to that of pure PNIPAM, at higher C_w it suddenly increases with temperature, thus indicating the formation of aggregates. The addition of PAAc, in fact, affects the delicate balance between hydrophobic and hydrophilic interactions. In particular, at this pH conditions (pH 5.5), where the fraction of deprotonated AAc is small but not negligible, the collapse of NIPAM networks above the VPTT is supposed to favor the exposure of PAAc dangling chains and interparticle interactions responsible for aggregation phenomenon.

The dynamical transition associated to the VPT is also observed in the temperature behaviour of the stretching parameter β of PNIPAM and IPN microgels reported in Fig.1(c),(d).

Moreover in the case of IPN intriguing differences depending on concentration are observed: for $C_w < 0.3$ % $\beta(T)$ decreases upon crossing the VPTT, while for $C_w > 0.3$ % the microgel collapse yields a sharp increase of the stretching coefficient. Therefore $C_w = 0.3$ % can be identified as the crossover concentration between two different behaviours emerging in IPN microgels at $C_{PAAc} = 23$ %. Both the τ and the β behaviours sign the existence of a concentration threshold ($C_w = 0.3$ %) above which

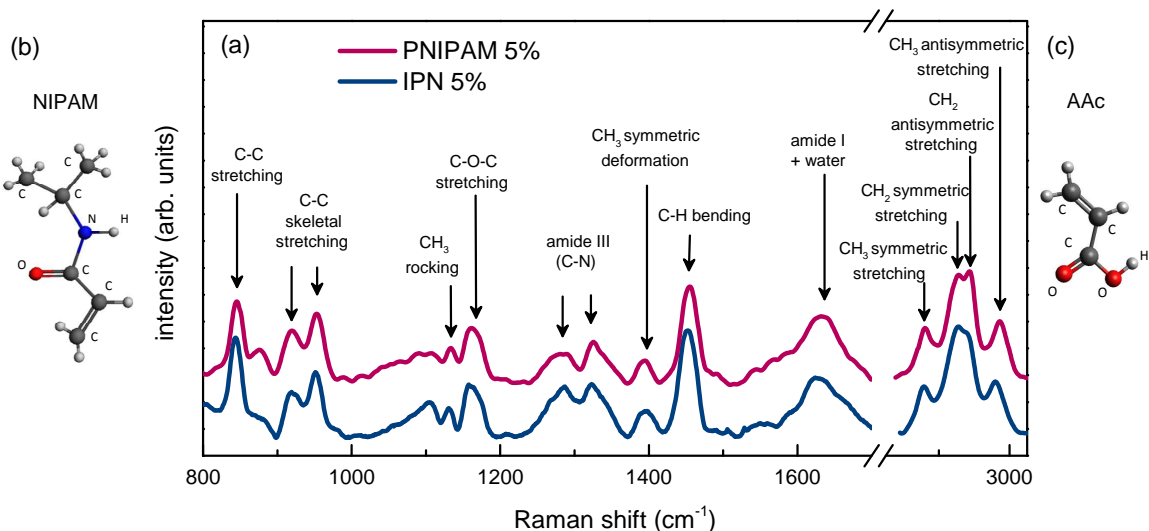


Figure 2: (a) Raman spectra for PNIPAM and IPN microgels at fixed temperature ($T=316\text{K}$) and concentration ($C_w=5\%$). (b)(c) Sketch of the NIPAM and AAc molecular structure.

interparticle interactions become important giving rise to aggregation.

To deeply investigate the molecular mechanism driving the VPT and the aggregation phenomenon, Dynamic Light Scattering measurements have been complemented with Raman spectroscopy on PNIPAM and IPN microgels at weight concentration equal and above the critical concentration $C_w=0.3\%$ to understand the role of the microgel hydration in the aggregation phenomena. Raman spectra over the frequency range from 800 to 3000 cm^{-1} for both PNIPAM and IPN microgels are reported in Fig. 2 together with the assignment of the principal vibrational modes. Interestingly PNIPAM and IPN microgels show quite similar Raman spectra corroborating the idea that their main features are associated to the C-C and C-H vibration bands, mainly derived from the NIPAM chain.

To investigate the structural changes induced by temperature we focus our attention on the spectral range between 2850 cm^{-1} and 3000 cm^{-1} , where bands ascribed to $\text{CH}_2\text{-CH}_3$ vibrations are present. The modifications in these vibrational modes, indeed, involve different interactions both among polymers and between polymers and water molecules, eventually shown by changes in $\text{CH}_2\text{-CH}_3$ bands, more sensitive to hydrogen bond variations [58]. Raman spectra of PNIPAM and IPN microgels at concentrations equal and greater to the critical weight concentration ($C_w=0.3\%$) are reported in Fig.3. In particular the initial and final states of the CH stretching vibrations due to the microgel shrinking have been determined from the steady state Raman spectra at temperatures below and above the VPTT (Fig.3(a,b,c,d)). Spectra have been deconvolved by four Gaussian contributions (Fig.3(e)), which can be assigned to different C-H stretching of the PNIPAM chain according to previous works in literature [65, 66]: symmetric stretching of CH_3 (2880 cm^{-1}), symmetric and antisymmetric stretching of CH_2

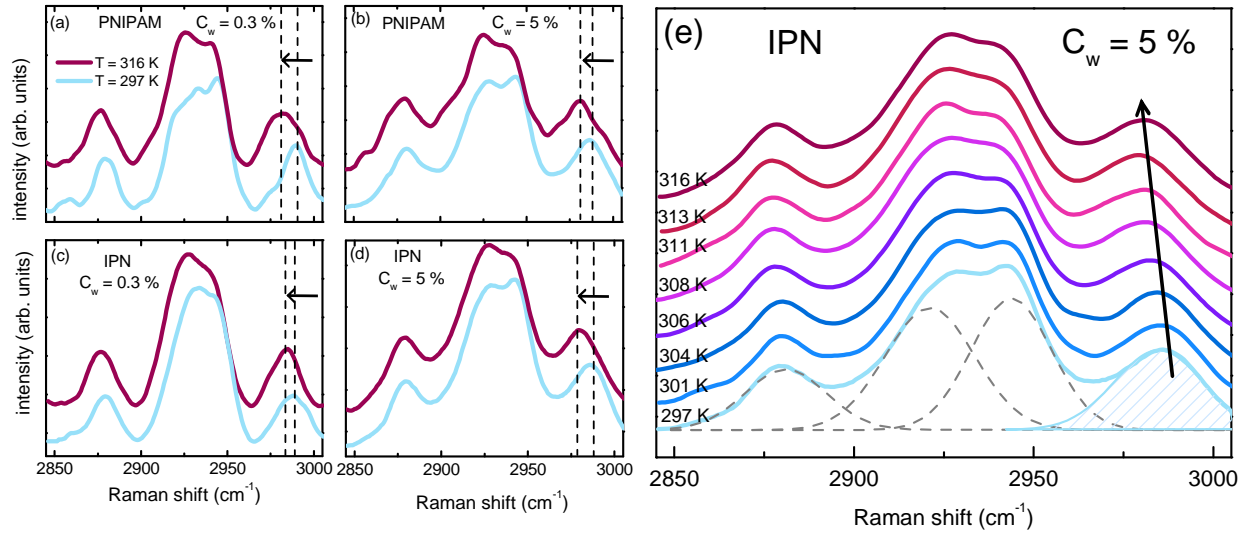


Figure 3: Raman spectra for (a)(b) PNIPAM and (c)(d) IPN microgels at temperature below (light cyan) and above (red) the VPTT, at $C_w=0.3\%$ and $C_w=5\%$. (e) Raman spectra for IPN microgels at $C_w=5\%$ at the indicated temperature values. The arrows highlight the frequency shift of CH_3 stretching band.

(2920 cm^{-1} , 2945 cm^{-1} respectively), antisymmetric stretching of CH_3 (2988 cm^{-1}).

Changes in the symmetric and antisymmetric CH_2 stretching modes and in particular their ratio have been related, in Ref.[67], to the lateral packing density of the polymer chain. Therefore in our case the increase of the symmetric CH_2 spectral weight upon crossing the VPTT can be ascribed to an increase of the packing density due to the coil-to-globule transition.

Additional details on the swelling behaviour can be obtained through the band related to the stretching vibration of CH_3 groups [65]. The whole temperature behaviour upon crossing the VPT is reported in Fig.3(e) for IPN microgels at $C_w=5\%$. At a glance the high frequency peak (2988 cm^{-1}) clearly exhibits a frequency red-shift upon crossing the VPTT, therefore the frequency of the CH_3 anti-symmetric stretching band is crucial to elucidate the molecular mechanism driving the swelling/shrinking behaviour of the microgel particles. With this aim the temperature behaviour of the peak frequency has been deeply investigated for both PNIPAM and IPN microgels: its behaviour for an aqueous suspension of PNIPAM microgels at $C_w=0.3\%$ is reported in Fig.4(a) and compared with the temperature behaviour of the hydrodynamic radius R_H in the high dilution limit. The frequency $\nu(T)$ decreases as temperature increases with a transition at temperature close to the VPTT, which can be mainly explained in terms of the hydration changes of the isopropyl side chain. As previously observed and theoretically investigated [68, 69], the higher number of water molecules surrounding the CH_3 groups correlates with the higher wavenumber of the CH_3 stretching vibration. Therefore this frequency shift following the temperature behaviour of the hydrodynamic radius endorses the idea that the volume

phase transition is accompanied by a reorganization of the water molecules leading to significative changes in the hydration.

For IPN microgels the scenario is more complex since the presence of PAAc affects the balance between hydrophilic and hydrophobic interactions and the net charge. As previously discussed, in this case a critical weight concentration is found at $C_w=0.3$ % where signatures of aggregation appear. The $\nu(T)$ behaviour for IPN microgels at $C_w=0.3$ % is reported in Fig.4(b) and compared with the temperature behaviour of the hydrodynamic radius R_H , to point out the volume phase transition of an IPN microgel. The decrease with temperature of the CH_3 frequency confirms that the main features of the PNIPAM shrinking are preserved. However an additional bump upon crossing the VPTT is observed, putting forward the idea that additional molecular mechanisms match with the microgel collapse. The smoother decrease of $\nu(T)$ observed in IPNs with respect to pure PNIPAM microgels allows to speculate that weaker H-bonds are involved in the coil-to-globule transition of the NIPAM chains making stronger the CH_3 bonds within the NIPAM chain. At these pH conditions (pH 5.5) indeed interactions between CONH and COOH groups belonging to PNIPAM and PAAc moieties are favored, making IPN microgel particle more hydrophobic than PNIPAM ones. Therefore introducing the PAAc within the PNIPAM network enhances the hydrophobicity of the microgel particles perturbing the role played by water molecules. This peculiar behaviour has to be related also to the interactions between IPN microgel particles that are indeed favored above the VPTT, in the shrunken state, where PAAc dangling chains are overexposed. In these conditions, H-bonds between COOH groups belonging to the AAc moieties or charge-like interactions are favored, affecting the typical transition to the shrunken dehydrated state.

These results suggest that most of the differences between PNIPAM and IPN microgel behaviours are expected to be strictly related to the interparticle interactions, to reinforce this evidence the temperature behaviour of the CH_3 antisymmetric stretching frequency has been investigated in the high concentration limit ($C_w=5$ %), where interactions between polymer chains belonging to different particles become more relevant due to close packing. The behaviours of $\nu(T)$ for both PNIPAM and IPN microgels at $C_w=0.3$ % and $C_w=5$ % are compared in Fig.5. For PNIPAM microgels no significative change is observed with concentration: for low (Fig.5(a)) and high (Fig.5(b)) concentrated samples a sharp decrease of $\nu(T)$ is observed at $T \approx 305$ K indicating that changes in the microgel dehydration mainly involve the CH_3 bondings. On the other hand, for IPN microgels the decrease of the frequency shift is accompanied by the characteristic bump above the VPTT which has been deeply discussed. However this bump becomes more evident at higher weight concentration, suggesting that the CH_3

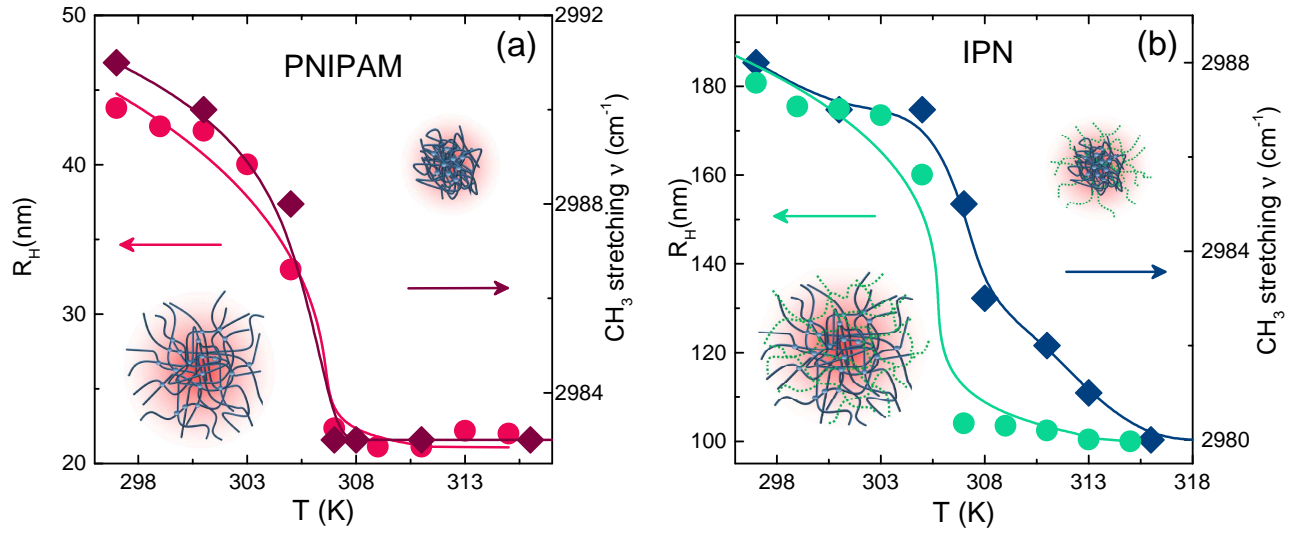


Figure 4: Hydrodynamic radius R_H and CH_3 frequency shift as a function of temperature for (a) PNIPAM and (b) IPN microgels. Magenta and green solid lines are the fit of $R_H(T)$ through the Flory-Rehner theory, red and blue solid lines are guide to eyes for the $\text{CH}_3(T)$ behaviour.

bonds get stronger due to the PAAc contribution as particles come into close contact. These results suggest that for IPN microgels two different molecular mechanisms drive the structural changes across the VPT, the first involving the coil-to-globule transition of the NIPAM chains and the latter driving the aggregation process supposedly due to the overexposure of the AAc chains.

4. Conclusions

The molecular mechanism driving the VPT and its influence on the microgel aggregation has been investigated by combining Dynamic Light Scattering and Raman spectroscopy. PNIPAM and IPN microgels have been investigated at low and high concentration, highlighting that in IPN microgels at $C_{\text{PAAc}} = 23\%$ a critical weight concentration ($C_w = 0.3\%$) exists above which aggregation phenomena become relevant. Raman measurements on both PNIPAM and IPN microgels clearly highlights that two different molecular mechanisms occur upon crossing the VPT. When the microgel particle goes towards the shrunken state, the number of H_2O molecules surrounding the CH_3 groups is reduced and the vibrational frequency of CH_3 stretching abruptly decreases. Indeed hydrophobic interactions are very similar for both PNIPAM and IPN microgels and the main features of the swelling behaviour are preserved. This peculiar behaviour is affected by interpenetrating the poly(acrylic acid) within the PNIPAM network and the balance between polymer/polymer and polymer/solvent interactions changes due to the PAAc network. In particular the presence of PAAc enhances the microgel hydrophobicity promoting interparticle interactions. The decrease of the frequency shift is characterized

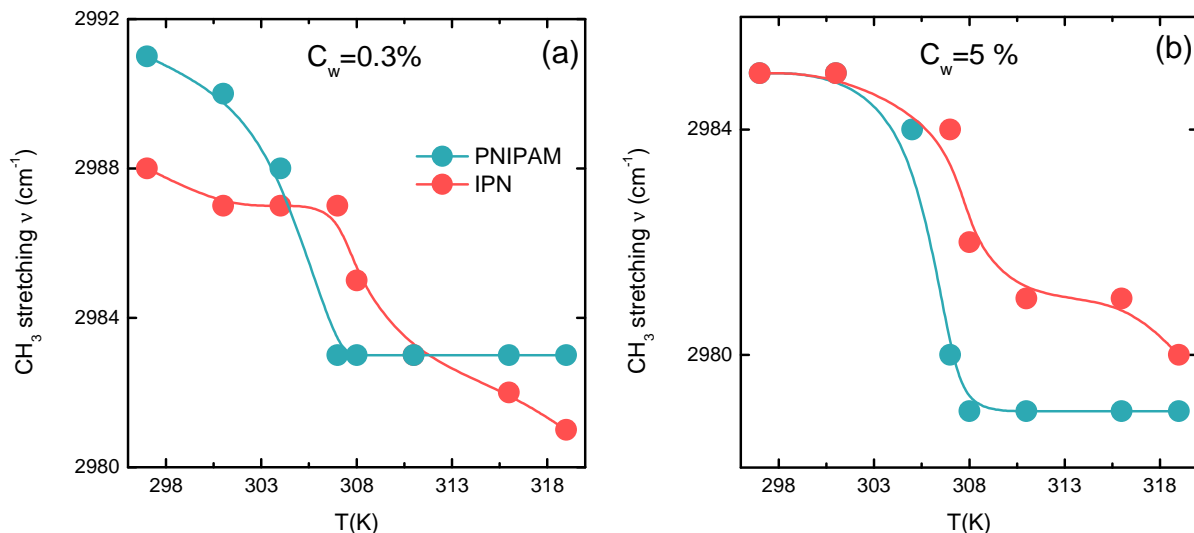


Figure 5: CH₃ frequency shift as a function of temperature for PNIPAM and IPN microgels at (a) $C_w = 0.3\%$ and (b) $C_w = 5\%$. Solid lines are guides to eyes.

by an unexpected double step decay across the VPT that becomes more relevant with increasing concentration, suggesting that two different mechanisms drive the structural changes across the VPT, the first involving the coil-to-globule transition of the NIPAM chains and the latter driving the aggregation process supposedly due to the overexposure of the AAc chains.

Acknowledgments

The authors acknowledge support from the European Research Council (ERC Consolidator Grant 681597, MIMIC) and from MIUR-PRIN (2012J8X57P).

Bibliography

References

- [1] L. A. Lyon and A. Fernandez-Nieves. The Polymer/Colloid Duality of Microgel Suspensions. *Annu. Rev. Phys. Chem.*, 63:25–43, 2012.
- [2] S. V. Vinogradov. Colloidal microgels in drug delivery applications. *Curr. Pharm. Des.*, 12:4703–4712, 2006.
- [3] M. Das, H. Zhang, and E. Kumacheva. MICROGELS: Old Materials with New Applications. *Annu. Rev. Mater. Res.*, 36:117–142, 2006.
- [4] J. S. Park, H. N. Yang, D. G. Woo, S. Y. Jeon, and K. H. Park. Poly(N-isopropylacrylamide-

- co-acrylic acid) nanogels for tracing and delivering genes to human mesenchymal stem cells. *Biomaterials*, 34:8819–8834, 2013.
- [5] M. Hamidi, A. Azadi, and P. Rafie. Hydrogel nanoparticles in drug delivery. *Adv. Drug Deliv. Rev.*, 60:1638–1649, 2008.
- [6] N. M. B. Smeets and T. Hoare. Designing Responsive Microgels for Drug Delivery Applications. *J. Polym. Sci. A Polym. Chem.*, 51:3027–3043, 2013.
- [7] S. Su, Ali Md. Monsur, C. D. M. Filipe, Y. Li, and R. H. Pelton. Microgel-Based Inks for Paper-Supported Biosensing Applications. *Biomacromolecules*, 9:935–941, 2008.
- [8] C. N. Likos, N. Hoffmann, H. Löwen, and A. A. Louis. Exotic fluids and crystals of soft polymeric colloids. *J. Phys. Cond. Matter*, 14:7681–7698, 2002.
- [9] P. E. Ramírez-González and M. Medina-Noyola. Glass transition in soft-sphere dispersions. *Journal of Physics: Condensed Matter*, 21(7):075101–13, 2009.
- [10] D.M. Heyes and A.C.Branka. Interactions between microgel particles. *Soft Matter*, 5:2681, 2009.
- [11] H. Wang, X. Wu, Z. Zhu, C. S. Liu, and Z. Zhang. Revisit to phase diagram of poly(N-isopropylacrylamide) microgel suspensions by mechanical spectroscopy. *J. Chem. Phys.*, 140:024908, 2014.
- [12] P. S. Mohanty, D. Paloli, J. J. Crassous, E. Zaccarelli, and P. Schurtenberger. Effective interactions between soft-repulsive colloids: Experiments, theory and simulations. *J. Chem. Phys.*, 140:094901, 2014.
- [13] T. Hellweg, C.D. Dewhurst, E. Brückner, K.Kratz, and W.Eimer. Colloidal crystals made of poly(N-isopropylacrylamide) microgel particles. *Colloid. Polym. Sci.*, 278:972–978, 2000.
- [14] J. Wu, B. Zhou, and Z. Hu. Phase behavior of thermally responsive microgel colloids. *Phys. Rev. Lett.*, 90(4):048304–4, 2003.
- [15] P. N. Pusey and W. van Megen. Phase behaviour of concentrated suspensions of nearly hard colloidal spheres. *Nature*, 320:340–342, 1986.
- [16] A. Imhof and J. K. G. Dhont. Experimental Phase Diagram of a Binary Colloidal Hard-Sphere Mixture with a Large Size Ratio. *Phys. Rev. Lett.*, 75:1662–1665, 1995.

- [17] K. N. Pham, A. M. Puertas, J. Bergenholtz, S. U. Egelhaaf, A. Moussaïd, P. N. Pusey, A. B. Schofield, M. E. Cates, M. Fuchs, and W. C. K. Poon. Multiple Glassy States in a Simple Model System. *Science*, 296:104–106, 2002.
- [18] T. Eckert and E. Bartsch. Re-entrant glass transition in a colloid-polymer mixture with depletion attractions. *Phys. Rev. Lett.*, 89:125701–4, 2002.
- [19] P. J. Lu, E. Zaccarelli, F. Ciulla, A. B. Schofield, F. Sciortino, and D. A. Weitz. Gelation of particle with short range attraction. *Nature*, 453:499–503, 2008.
- [20] C. P. Royall, S. R. Williams, T. Ohtsuka, and H. Tanaka. Direct observation of a local structural mechanism for dynamical arrest. *Nat. Mater.*, 7:556–561, 2008.
- [21] B. Ruzicka, E. Zaccarelli, L. Zulian, R. Angelini, M. Sztucki, A. Moussaïd, T. Narayanan, and F. Sciortino. Observation of empty liquids and equilibrium gels in a colloidal clay. *Nat. Mater.*, 10:56–60, 2011.
- [22] R. Angelini, E. Zaccarelli, F. A. de Melo Marques, M. Sztucki, A. Fluerasu, G. Ruocco, and B. Ruzicka. Glass-glass transition during aging of a colloidal clay. *Nat. Commun.*, 5:4049–7, 2014.
- [23] R. H. Pelton and Chibante P. Preparation of aqueous lattices with N-isopropylacrylamide. *Colloids Surf.*, 20:247–256, 1986.
- [24] J. Wu, G. Huang, and Z. Hu. Interparticle Potential and the Phase Behavior of Temperature-Sensitive Microgel Dispersions. *Macromolecules*, 36:440–448, 2003.
- [25] V. Nigro, R. Angelini, M. Bertoldo, and B. Ruzicka. Swelling of responsive-microgels: experiments versus models. *Colloids Surf. A*, 532:389–396, 2017.
- [26] J. J. Lietor-Santos, B. Sierra-Martin, R. Vavrin, Z. Hu, U. Gasser, and A. Fernandez-Nieves. Deswelling Microgel Particles Using Hydrostatic Pressure. *Macromolecules*, 42:6225–6230, 2009.
- [27] K. Kratz, T. Hellweg, and W. Eimer. Structural changes in PNIPAM microgel particles as seen by SANS, DLS and EM techniques. *Polymer*, 42:6631–6639, 2001.
- [28] P.J. Flory. *Principles of Polymer Chemistry*. Cornell University, Ithaca, New York, 1953.
- [29] A.K. Lele, M.M. Hirve, M.V. Badiger, and R.A. Mashelkar. Predictions of bound water content in poly (N-isopropylacrylamide) gel. *Macromolecules*, 30:157–159, 1998.

- [30] T. Hino and J. M. Prausnitz. Swelling Equilibria for Heterogeneous Polyacrylamide Gels. *J. Appl. Polym. Sci.*, 62:1635–1640, 1996.
- [31] K. Otake, H. Inomata, M. Konno, and S. Saito. Thermal-analysis of the volume phase-transition with N-Isopropylacrylamide gels. *Macromolecules*, 23:283–289, 1990.
- [32] T. Lòpez-Leòn and A. Fernandez-Nieves. Macroscopically probing the entropic influence of ions: deswelling neutral microgels with salt. *Phys. Rev. E*, 75:011801, 2007.
- [33] J. Mattsson, H. M. Wyss, A. Fernandez-Nieves, K. Miyazaki, Z. Hu, D. Reichman, and D. A. Weitz. Soft colloids make strong glasses. *Nature*, 462(5):83–86, 2009.
- [34] D. Paloli, P. S. Mohanty, J. J. Crassous, E. Zaccarelli, and P. Schurtenberger. Fluid–solid transitions in soft-repulsive colloids. *Soft Matter*, 9:3000–3004, 2013.
- [35] B. H. Tan, R. H. Pelton, and K. C. Tam. Microstructure and rheological properties of thermo-responsive poly(N-isopropylacrilamide) microgels. *Polymers*, 51:3238–3243, 2010.
- [36] P. W. Zhu and D. H. Napper. Light scattering studies of poly(N-isopropylacrylamide) microgel particle in mixed water-acetic acid solvents. *Macromol. Chem. Phys.*, 200:1950–1955, 1999.
- [37] K. Kratz and W. Eimer. Swelling Properties of Colloidal Poly(N-Isopropylacrylamide) Microgels in Solution. *Ber. Bunsenges. Phys. Chem.*, 102:848–854, 1998.
- [38] T. Hellweg, C. D. Dewhurst, W. Eimer, and K. Kratz. PNIPAM-co-polystyrene core-shell microgels: structure, swelling behavior, and crystallization. *Langmuir*, 20:4333–4335, 2004.
- [39] Z. Meng, J. K. Cho, S. Debord, V. Breedveld, and L. A. Lyon. Crystallization Behavior of Soft, Attractive Microgels. *J. Phys. Chem. B*, 111:6992–6997, 2007.
- [40] K. Kratz, T. Hellweg, and W. Eimer. Influence of charge density on the swelling of colloidal poly(N-isopropylacrylamide-co-acrylic acid) microgels. *Colloids Surf. A*, 170:137–149, 2000.
- [41] K. Kratz, T. Hellweg, and W. Eimer. Effect of connectivity and charge density on the swelling and local structure and dynamic properties of colloidal PNIPAM microgels. *Ber. Bunsenges. Phys. Chem.*, 102(11):1603–1608, 1998.
- [42] X. Xia and Z. Hu. Synthesis and Light Scattering Study of Microgels with Interpenetrating Polymer Networks. *Langmuir*, 20:2094–2098, 2004.

- [43] C. D. Jones and L. A. Lyon. Synthesis and Characterization of Multiresponsive Core-Shell Microgels. *Macromolecules*, 33:8301–8303, 2000.
- [44] V. Nigro, R. Angelini, M. Bertoldo, V. Castelvetro, G. Ruocco, and B. Ruzicka. Dynamic light scattering study of temperature and pH sensitive colloidal microgels. *J. Non-Cryst. Solids*, 407:361–366, 2015.
- [45] V. Nigro, R. Angelini, M. Bertoldo, F. Bruni, M.A. Ricci, and B. Ruzicka. Local structure of temperature and ph-sensitive colloidal microgels. *J. Chem. Phys.*, 143:114904–9, 2015.
- [46] Z. Hu and X. Xia. Hydrogel nanoparticle dispersions with inverse thermoreversible gelation. *Adv. Mater.*, 16(4):305–309, 2004.
- [47] J. Ma, B. Fan, B. Liang, and J. Xu. Synthesis and characterization of Poly(N-isopropylacrylamide)/Poly(acrylic acid) semi-IPN nanocomposite microgels. *J. Colloid Interface Sci.*, 341:88–93, 2010.
- [48] W. Xiong, X. Gao, Y. Zao, H. Xu, and X. Yang. The dual temperature/pH-sensitive multiphase behavior of poly(Nisopropylacrylamide-co-acrylic acid) microgels for potential application in *in situ* gelling system. *Colloids Surf. B: Biointerfaces*, 84:103–110, 2011.
- [49] L. A. Lyon, J. D. Debord, S. B. Debord, C. D. Jones, J. G. McGrath, and M. J. Serpe. Microgel Colloidal Crystals. *J. Phys. Chem. B*, 108:19099–19108, 2004.
- [50] P. Holmqvist, P. S. Mohanty, G. Nägele, P. Schurtenberger, and M. Heinen. Structure and Dynamics of Loosely Cross-Linked Ionic Microgel Dispersions in the Fluid Regime. *Phys. Rev. Lett.*, 109:048302–5, 2012.
- [51] S. B. Debord and L. A. Lyon. Influence of Particle Volume Fraction on Packing in Responsive Hydrogel Colloidal Crystals. *J. Phys. Chem. B*, 107:2927–2932, 2003.
- [52] X. Xia, Z. Hu, and M. Marquez. Physically bonded nanoparticle networks: a novel drug delivery system. *J. Control. Release*, 103:21–30, 2005.
- [53] J. Zhou, G. Wang, L. Zou, L. Tang, M. Marquez, and Z. Hu. Viscoelastic Behavior and In Vivo Release Study of Microgel Dispersions with Inverse Thermoreversible Gelation. *Biomacromolecules*, 9:142–148, 2008.

- [54] Z. Xing, C. Wang, J. Yan, L. Zhang, L. Li, and L. Zha. pH/temperature dual stimuli-responsive microcapsules with interpenetrating polymer network structure. *Colloid Polym. Sci.*, 288:1723–1729, 2010.
- [55] X. Liu, H. Guo, and L. Zha. Study of pH/temperature dual stimuli-responsive nanogels with interpenetrating polymer network structure. *Polymers*, 61(7):1144–1150, 2012.
- [56] Z. Ahmed, E.A. Gooding, K.V. Pimenov, L. Wang, and S.A. Asher. Uv resonance raman determination of molecular mechanism of poly(n-isopropylacrylamide) volume phase transition. *J. Chem. Phys. B*, 113:4248–4256, 2009.
- [57] M.H. Futscher, M. Philipp, P. Müller-Buschbaum, and A. Schulte. The Role of Backbone Hydration of Poly(N-isopropyl acrylamide) Across the Volume Phase Transition Compared to its Monomer. *Scientific Reports*, 7(17012):1–10, 2017.
- [58] T. Wu, A.B. Zrimsek, S.V. Bykov, R.S. Jakubek, and S.A. Asher. Hydrophobic Collapse Initiates the Poly(N-isopropylacrylamide) Volume Phase Transition Reaction Coordinate. *The Journal of Physical Chemistry B*, 122(11):3008–3014, 2018.
- [59] R. Kohlrausch. Theorie des elektrischen rckstandes in der leidener flasche. *Annalen der Physik*, 2, 1854.
- [60] G. Williams and D. C. Watts. Non-Symmetrical Dielectric Relaxation Behavior Arising from a Simple Empirical Decay Function. *J. Chem. Soc. Faraday Trans.*, 66:80–85, 1970.
- [61] A.L. Glebov, O. Mokhun, A. Rapaport, S. Vergnole, V. Smirnov, and L. B. Glebov. Volume bragg gratings as ultra-narrow and multiband optical filters. *Proc. of SPIE*, 8428:84280C–4, 2012.
- [62] F. Capitani, S. Koval, R. Fittipaldi, S. Caramazza, E. Paris, W. S. Mohamed, J. Lorenzana, A. Nucara, L. Rocco, A. Vecchione, P. Postorino, and P. Calvani. Raman phonon spectrum of the Dzyaloshinskii-Moriya helimagnet $Ba_2CuGe_2O_7$. *Phys. Rev. B*, 91:214308, 2015.
- [63] J. Gapinski and A. Patkowski and A. J. Banchio and J. Buitenhuis and P. Holmqvist and M. P. Lettinga and G. Meier and G. Nägele. Structure and short-time dynamics in suspensions of charged silica spheres in the entire fluid regime. *J. Chem. Phys*, 130:084503, 2009.
- [64] A. J. Banchio and G. Nägele. Short-time transport properties in dense suspensions: From neutral to charge-stabilized colloidal spheres. *J. Chem. Phys*, 128:104903, 2008.

- [65] J. Dybal, M. Trchova, and P. Schmidt. The role of water in structural changes of poly(n-isopropylacrylamide) and poly(n-isopropylmethacrylamide) studied by ftir, raman spectroscopy and quantum chemical calculations. *Vibrational Spectroscopy*, 51:44–51, 2009.
- [66] Y. Tsuboi, M. Nishino, and N. Kitamura. Laser-induced reversible volume phase transition of a poly(n-isopropylacrylamide) gel explored by raman microspectroscopy. *Polymer Journal*, 40:367–374, 2008.
- [67] M. Pastorczak, M. Kozanecki, and J. Ulanski. Water-Polymer interactions in PVME hydrogels - Raman spectroscopy studies. *Polymer*, 50(19):4535 – 4542, 2009.
- [68] P. Schmidt, J. Dybal, and M. Trchova. Investigations of the hydrophobic and hydrophilic interactions in polymer-water systems by atr ftir and raman spectroscopy. *Vibrational Spectroscopy*, 42:278–283, 2006.
- [69] P. Hobza and Z. Havlas. Improper, blue-shifting hydrogen bond. *Theoretical Chemistry Accounts*, 108(6):325–334, Dec 2002.